Study of High DC Voltage breakdown between stainless steel electrodes separated by long vacuum gaps

N. Pilan[*1], S. M Deambrosis[3], A. De Lorenzi[1], M. Fincato[1], C. Fontana[2], R. Gobbo[2], L. Lotto[2], E. Martines[1], O. Mc Cormack[4], R. Pasqualotto[1], T. Patton[1,2], G. Pesavento[2], F. Pino[2], E. Spada[1], S. Spagnolo[1], and M. Zuin[1].

[1]Consorzio RFX, Associazione EURATOM-ENEA sulla Fusione, Corso Stati Uniti 4, 35127 Padova, Italy
[2]Università di Padova, Italy
[3]ICMATE CNR ,Padova , Italy
[4] INFN ,Milano , Italy

Abstract.

HV insulation across a single gap in vacuum and low-pressure gas is a critical issue in relation to the development and realization of the electrostatic accelerator for the ITER Neutral Beam Injector (NBI) [1].
The present paper describes and analyzes the recent experimental results obtained at the High Voltage Padova Test Facility (HVPTF), the laboratory aimed at supporting the development of the prototype for the ITER NBI [2].
A voltage up to 800kV_{DC} was achieved in the HVPTF during the experimental campaigns with a sphere-plane configurations having variable gap length (from 30 to 150 mm) and pressure ranging from high vacuum (10^{-7} mbar) to 10^{-3} mbar in Argon.
Such an experimental campaign represents one of the few examples where voltages higher than 500-550 kV DC are sustained by a single vacuum gap between electrodes [3] and therefore constitutes additional experience to improve the knowledge of voltage holding across large vacuum gaps.
The results in high vacuum indicate that at the beginning of voltage conditioning the breakdown events occur at the same cathodic electric field irrespective of the electrode geometry. However, after sufficient conditioning time, the breakdown voltage distribution seems to depend also on the electric field at the anode and on the total voltage between electrodes.
A benchmark between a numerical tool previously developed to predict the voltage holding in high vacuum (Voltage holding Prediction Model, VHPM [4]) and the experimental results is also reported and discussed.

1. Introduction

The program dedicated to the construction and commissioning of MITICA, which is the full size prototype of the Negative-ion based Neutral Beam Injector (NBI) for ITER [1], is complemented by intense R&D activity on high-voltage insulation in vacuum.
The ITER NBI is devoted to the injection of a D neutral beam in the ITER plasma to obtain breakeven conditions. These conditions will be achieved by delivering a neutral beam with a stationary power of 16.5 MW lasting for one hour (duty cycle 1:3) and with a particle energy of 1 MeV.
The NBI consists of a negative ion Beam Source (BS), a 1 MeV electrostatic accelerator, a neutralizer, a residual ion dump and a diagnostic calorimeter. The rated negative ion currents at the exit of the electrostatic accelerator are 40 A (for D^-) and 46 A (for H^-) [5] [6] . The ion current is extracted from a large Radio Frequency (RF) cesiated ion source [7].

The MITICA electrostatic configuration is much more complex than any NBI ever realized, and the accelerating voltage of 1 MV will be twice the voltage so far achieved [8]. The main reason of such complexity is due to the fact that the whole Beam Source and Accelerator will be insulated using a vacuum instead of using an insulating gas (e.g. SF_6). This design choice has avoided Radiation-Induced Conductivity (RIC) [9] [10] effects in SF_6, in the presence of neutrons and γ radiation produced by fusion reactions, but has introduced some risks concerning the voltage holding of the MITICA BS insulation. For this reason, R&D work on voltage insulation in vacuum is necessary to secure a stable hold voltage.
Figure 1 shows a vertical cross section of the BS inside the BS Vessel (BSV). The system is a cantilever structure whose load is supported from the Grounded Grid (GG) potential by means of 96 alumina insulators represented in Figure 1 by cyan cylinders.
The bottom view of Figure 1 shows a horizontal cross section of the ion source followed by the multi-stage electrostatic accelerator. The electrostatic accelerator is composed of 5 electrodeposited copper grids, namely $AG_{i\,(i=1\ldots4)}$, each grid has 1280 apertures; the accelerating grids are polarized respectively at -0.8, -0.6, -0.4 and -0.2 MVdc with respect to grounded vessel.
The large cathodic surface (~10 m^2) of Figure 1 highlighted in green is a stainless steel electrostatic screen, this envelops the rear part of the ion source and the top connections to the High Voltage Bushing (HVB). The screen is polarized at -1 MVdc and insulated from the ground by vacuum gaps longer than 950 mm. A number of smaller stainless steel electrodes - the screens of the supporting structures, the screens of the alumina insulators, the grid cooling pipes and the HVB screens - are located inside the BSV and exposed to electric fields from 1 to a few tens of kV/mm.

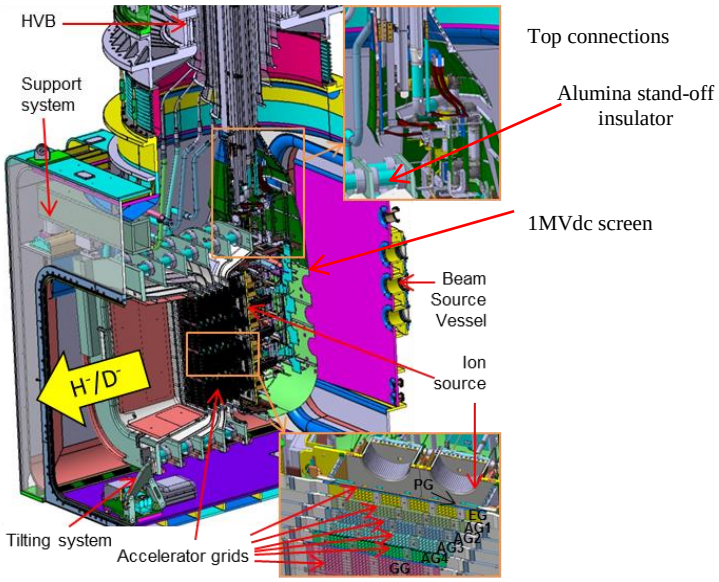

Figure 1. Vertical Section of the MITICA vacuum vessel and beam source (left) and horizontal section of the ion source and electrostatic accelerator (right).

The vacuum level inside the BSV has an influence on voltage holding. The H_2/D_2 pressure ranges from 10^{-5} to 10^{-2} Pa [11], depending on the operating conditions.
This region around the BS is not separated from the vacuum between the accelerating grids, nor is it separated from the RF plasma volume and the vacuum in the rear part of the BS between the RF coils and the 1MV screen. The pressure distribution is governed by the conductance between the accelerating grids and the lateral apertures of the electrostatic accelerator [11]; this means that the gas pressure inside the beam source varies from place to place and can influence the hold-off voltage in various places depending on the local value of the Paschen *pd* parameter [12].

At present knowledge, on the basis of the recent results obtained in SPIDER - the Ion Source experiment aimed at optimizing the uniformity of the D^- and H^- beam before the operation in MITICA [13] - and the experience gained on other current and previous negative ion accelerators [8] [14], four operating condition are identified to be attained in sequence up to the beam-on status.

- The first working condition corresponds to the application of dc voltage in high vacuum ($p<10^{-3}$ Pa). Full insulation capability in high vacuum can be achieved after a relatively long conditioning procedure. The high voltage conditioning procedure is an in situ treatment to quench any possible sources of breakdown, the voltage is increased steadily (ramps or small steps) in such a way that the pre-breakdown currents, desorbed gasses and X ray emissions tend to extinguish or stabilize between each consecutive step. Above a certain value the voltage cannot be further increased. An estimation of the hold-off voltage in MITICA in high vacuum was done numerically in [15] and in [16]. These analyses indicated a maximum hold-off voltage of 600 - 800 kV_{dc} with the vacuum gap length in the range 60 – 100 cm. These results depend mainly on the total voltage effect [17] [3] that predicts a strong nonlinear dependence of the voltage breakdown on the gap length. Actually, for long gaps the voltage breakdown shows the tendency to saturate with the gap length; so far there is no experimental evidence that a voltage of 1MV dc can be sustained by a single high vacuum gap, and for lengths up to 1290 mm it has only been possible to sustain up to 705 kV in high vacuum [18]. On the other hand, it has been demonstrated that 1 MV is achievable by adopting a multi-stage structure [18] [19].

- The second corresponds to the introduction of H_2 (or D_2) in the Ion Source and to the application of Radio Frequency (RF) voltage at 1MHz to generate the plasma by means of the driver coils. This should be done at the end of the conditioning procedure described in the previous point; during this phase the beam is not accelerated, i.e. the DC voltage is set to zero. During this phase the RF coils located in the rear part of the BS could also cause electric discharges both in high and medium vacuum depending on the combination of RF power and gas pressures [13]. A pressure in the range 0.1 - 1.0 Pa is expected in the plasma source for the production and extraction of the required current of negative ions; in this condition the pressure in the region surrounding the beam source should be in the range 10^{-2} - 10^{-1} Pa.

- The third working condition is the application of the full voltage in presence of the gas inside the beam source vessel, but with RF coils inactive. In this case, an improvement of the DC hold-off voltage is expected, due to the so called “pressure effect” phenomenon [20] [17] [3] [12] [21]The voltage holding improvement should be observed once the pressure around the BS is kept at $\approx 10^{-2}$ Pa, a pressure compatible with the ones expected during the beam extraction. Although much experimental evidence describing this behavior is available in literature, neither consolidated physical explanations nor reliable numerical models are presently available to predict numerically such an improvement, so the real effectiveness of this method can be verified only on the accelerator prototype. It must be pointed out that even if the use of the pressure effect improves the voltage holding, a Townsend discharge can occur if the pressure exceeds the limit of $\sim 10^{-1}$ Pa [9] . In fact, in the region surrounding the electrostatic accelerator, where the gap is ≈ 1 m, the product of the pressure times the gap length is $pd \sim 10^{-1}$ [Pa·m], corresponding to the left branch of the Paschen curve for H_2 (or D_2).

- The final working condition corresponds to the extraction and acceleration of the nominal negative ion current. In this phase, according with the experience reported in [8], each stage of the electrostatic accelerator is energized at the nominal voltage, the RF will be activated and eventually the extraction grid will be activated. A sufficient margin between the nominal voltage and the voltages obtained in conditions #1 and 3 should guarantee a stable acceleration of the negative ion beam to the design parameters. This step has the highest probability of breakdowns, actually this working condition includes all the phenomena described in the previous points. Moreover the presence of a high heat flux on the accelerating grid surfaces could induce sputtering phenomena and diffusion of metal vapors. The presence of Cs and the high rate of X and gamma rays caused by the bremsstrahlung radiation due to the

stripped electrons along the beam path are additional aspects which can limit the energy of the accelerated beam.

The overview on voltage holding in a vacuum for MITICA presented so far outlines the different challenges to be solved to guarantee the achievement of the MITICA targets. It's now common understanding that the voltage holding issues can be fully addressed only in MITICA: in fact, the R&D on voltage holding is part of the MITICA experimental program.
Nevertheless, the R&D on smaller HV facilities – e.g. the 800 kV High Voltage Padova Test Facility (HVPTF) [2] - is a strategic activity to study the fundamental processes leading to breakdown, aimed at developing new diagnostics, new models and new modes of operation addressed to effectively guarantee a stable acceleration voltage in MITICA.

This paper deals with the results recently obtained at the HVPTF. The experimental campaigns were aimed to clarify aspects related to the first and the third working conditions mentioned above. The results of four experimental campaigns on stainless steel electrodes are reported and discussed.

2. Experimental apparatus and method

2.1 Experimental Apparatus

The system (Figure 2) consists of a cylindrical vacuum chamber (stainless steel AISI304, diameter 1200 mm, length 2400 mm). The vacuum chamber is evacuated by a turbomolecular pump 1 m^3/s baked by a dry scroll pump 0.16 m^3/s. A gas flux can be introduced by a manual micrometric valve; the pressure can be stably controlled in the range from 10^{-4} to 1.0 [Pa].

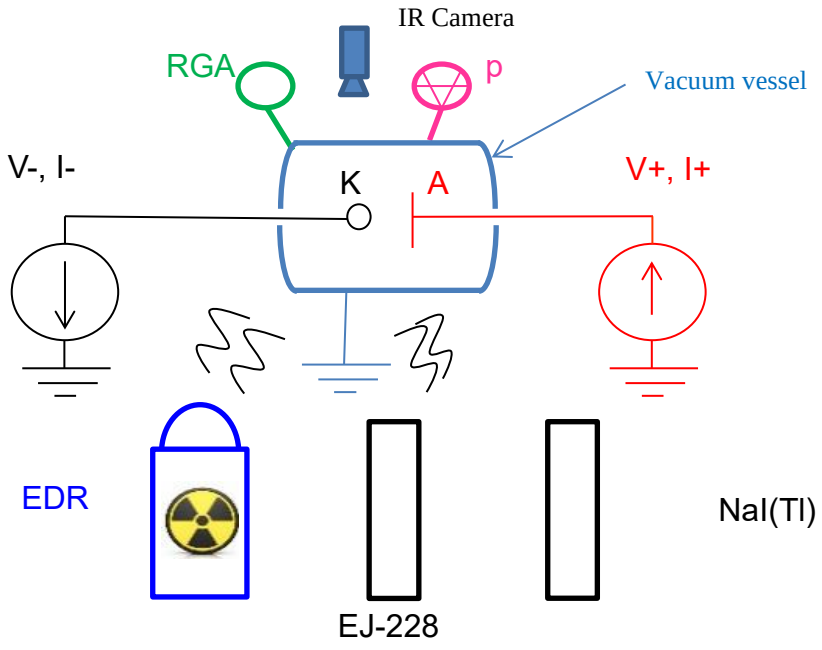

Figure 2 Experimental setup scheme and measured quantities. V+, I+ and V-, I- are the measured voltage and currents respectively for the positive and negative power supply; Residual Gas Analyzer (RGA) is the mass spectrometer; p is the pressure gauge; EDR represents the X (and gamma) ray dosimeter to measure the Equivalent Dose Rate; EJ-228 and NaI(TI) represent the scintillator probes.

The two K (cathode) and A (anode) electrodes (Figure 2) are arranged to make experiments with gaps from a few millimeters to ~250 mm. The electrodes are disk-shaped, with a Rogowsky profile, with different diameters and spheres of various radii. Exposed to vacuum are the two electrodes under test, the inner wall of the vacuum chamber (AISI304), the glass-covered surface of the insulators, and the vacuum sealing made by copper or Viton™.
Two Cockcroft-Walton Power Supplies (PS), rated +400 and -400 kV_{dc}/1 mA, are connected to the electrodes by means of XLPE insulated unipolar cables with screens that are terminated on SF_6-to-vacuum alumina feedthrough. The highest voltage achievable between the electrodes is therefore 800 kV_{dc}. Each feedthrough supports the K and A electrodes through a stainless steel extension equipped with electrostatic stress rings. The simplified electrical scheme of the system is shown in Figure 3: each power supply has an equivalent capacitance of C_2 = 2.7 nF and resistance R_2 = 15 MOhm; the output voltage is measured through the R_3 = 4 GOhm voltage divider; the output resistor R_1 = 15 MOhm decouples the PS from the load. The HV cables are 3 m long, inner diameter 10 mm, outer diameter 44 mm. Both HV cables have an equivalent capacitance of C_1 = 0.22 nF, and inductance L = 0.3 μH with negligible resistance. The electrodes have a ground capacitance and gap capacitance C_{el} of a few pF.

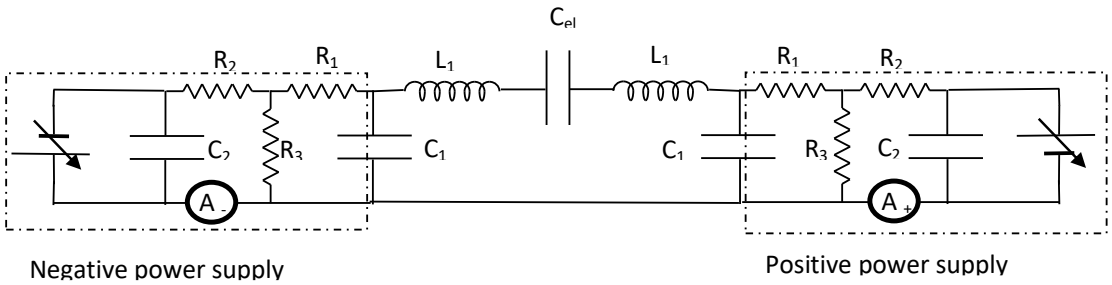

Figure 3. Equivalent electrical scheme of the HV circuit.

The current and voltage of each PS are measured with a bandwidth of about 1 kHz. The imbalance between I_{pos} and I_{neg} is the net current flowing to the vacuum chamber acting as the third electrode. The pressure signal p is acquired by a Bayard Alpert hot-cathode gauge (Oerlikon ITR90). The Equivalent Dose Rate (EDR) [μSv/h] of the X-rays produced during the experiment is measured by a Berthold Dose Rate Probe LB 1236 located outside the vacuum chamber, 1 meter from the chamber wall. Current, Voltage, Pressure signals are sampled at 100 Hz. The Residual Gas Analyzer (RGA) is an Inficon TS100 1-100 amu. The signals of each mass are sampled in sequence every 2 seconds.
The setup is equipped with an acquisition system calibrated to detect the energy spectra of the x-rays emitted during the voltage application. The system consists of two scintillators: a NaI(Tl) inorganic scintillator, 76 mm in diameter and 51 mm thick, and a EJ-228 organic scintillator made of Polyvinyltoluene (PVT), 51 mm in diameter and 51 mm thick positioned outside the vacuum chamber, 1 meter away from a glass window DN 100, 5 mm thick. Each scintillator is coupled with its own photomultiplier and connected to a CAEN DT5720B multichannel digitizer: the energy and time of each single photon detected is recorded up to a maximum rate of 350 kHz.

2.2 Electrode description

The electrode material is stainless steel AISI 304. The surface roughness is better than 0.4 μm, obtained using abrasive papers with abrasive grains of aluminum oxide, dimensions from 12 to 3 μm. Electrodes are cleaned in a water solution with an alkaline detergent by using an ultrasonic bath; they are then rinsed with acetone and

Figure 4. Picture of stainless steel electrodes adopted for the HV tests: sphere ϕ 24 mm, sphere ϕ40 mm, and plane ϕ108 mm.

wiped with clean cloths.

Table I reports the geometric configurations of the electrodes adopted in the experimental campaigns described in Section 3.

Table I. Geometric configurations used in the tests.

Configuration #	Cathode	Anode	Gap length [mm]
C#1	Sphere ϕ 40 mm	Plane ϕ108 mm	33
C#2	Sphere ϕ 40 mm	Plane ϕ108 mm	72
C#3	Sphere ϕ 40 mm	Plane ϕ108 mm	147
C#4	Sphere ϕ 24 mm	Sphere ϕ 24 mm	30

2.3 Experimental procedure

The high voltage tests for each configuration reported in table I were carried out in two phases: the first corresponds to the high voltage conditioning in high vacuum at a pressure lower than 10^{-6} mbar , the second phase corresponds to the "pressure effect" test.

2.3.1 High voltage tests in high vacuum

It must be pointed out that in these kinds of experiments the reproducibility is far from being attained [3] – even with the exact same electrode configuration and materials - due to the intrinsic difficulty to control the characteristics of the materials exposed to vacuum [22] and the effects produced by the conditioning process (influenced by the procedure employed and by the stored energy). Because of this, considerable efforts have been devoted to control the preparation of the tests to the highest degree feasible, in order to keep the characteristics of the metal-vacuum interfaces constant for as long as possible. A reproducibility test has been carried out on configuration #1, described in the Experimental Results section.
In all cases, the voltage was applied anti-symmetrically, driving both PS with the same reference voltage (V_{pos} = $-V_{neg}$), with a current limit for both PS set to $I_{pos} = -I_{neg} = 0.3$ mA. To get rid of the uncertainty due to the manually-operated voltage conditioning, an automatic conditioning procedure described in Figure 5 has been applied [23].

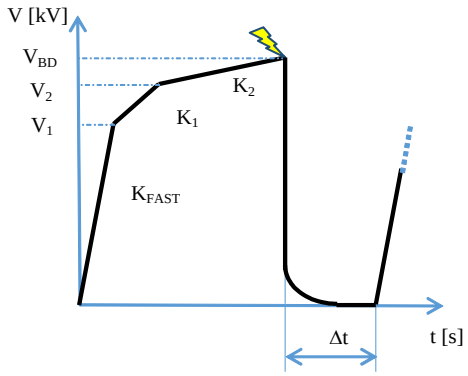

Figure 5 Time evolution of voltage applied during the automatic conditioning procedure.

1. After the breakdown event, the two PS are switched off and then switched on after the Δt period. Δt= 120 s
2. Ramp up to voltage $V_{1\,i+1}=0.9 \cdot V_{BD\,i}$ rate of rise K_{FAST}=50 kV/min
3. Ramp up to voltage $V_{2\,i+1}=V_{BD\,i}$ rate of rise K_1= 1.0 kV/min
4. Ramp up to voltage breakdown $V_{BD\,i+1}$ rate of rise K_2=0.5 kV/min

Starting voltage of the sequence V_{BD1}=160 kV.

The procedure is applied until the average V_{BD} remains constant; this occurs after at least 200 breakdowns. The HV tests are carried out continuously for 8 - 10 hours per day, and the conditioning finishes after 10 - 12 days. During the night the voltage conditioning is stopped, but the vacuum level is maintained.

2.3.2 High voltage tests in medium vacuum

At the end of the conditioning procedure in high vacuum the “pressure effect” was tested for each configuration mentioned in table I. The tests have been carried out by injecting a gas flux according to the desired pressure. For each pressure the voltage has been raised applying a symmetric distribution of voltages (V_{pos}=V_{neg}), starting from zero, with a rate of 50kV/min up to the breakdown occurrence. The test was repeated for each electrostatic configuration, increasing the pressure step by step up to the value for which the breakdown voltage drops below the voltage w/o gas injection (a clear indication that the left branch of the Paschen curve has been intercepted). From this point on the procedure is repeated, reducing the pressure in the inverse sequence.

3. Experimental results

3.1 Reproducibility tests

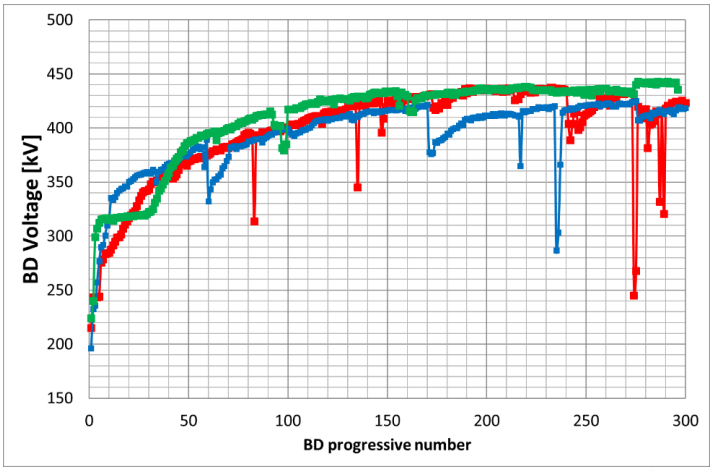

Figure 6- Breakdown voltage vs. breakdown progressive number, during 3 repetitions of test C#1 of Table I, red curve: 1st test, blue curve: 2nd test (5 weeks after 1st), green curve (17 weeks after 2nd) :

Before the initiation of the experimental campaign, a reproducibility test has been carried out. The tests consisted in the application of the voltage conditioning procedure reported in fig. 5 on three sets of identical electrodes (same material, same treatment procedure) with reference to the C#1 of Table I. In between these tests, different experimental campaign were carried out in the HVPTF; (the second test was performed 5 weeks after the first test and the third test 17 weeks after the second).
The conditioning histories show very similar behavior until BD #170, where the highest voltage is reached for the first and second sessions, at the (average) value of 425 kV; after this point, deconditioning events started to occur in the second (@ #170) and in first session (@ #240), whilst the third session didn't suffered from any deconditioning, reaching the highest value of 440 kV. Nevertheless, within some tens of breakdowns after the deconditioning event, all sessions converged to the same values. The conclusion is that the procedure employed in this setup gives reproducible results within a scattering of ±6% on the final BD voltages.

3.2 Analysis of the phenomenology

Figure 7- shows the typical phenomenology that appears during voltage conditioning when the voltage is applied using the procedure described in Figure 5. Over long timescale (>350 s), we clearly see a systematic correspondence among the voltage application, the appearance of a train of current burst (a), a pressure increase (b), and X-ray emission (c – dose rate); in (d) the X-ray energy spectra measured by the EJ228 scintillator is also reported.

The RGA signals are in line with the pressure signals. Although the dominant signal is water (18), the gases desorbed during conditioning are: H2 (2), N2 (28) and CO2 (44).
A transition between stationary filed emission currents and unstable microdischarges can be observed while the applied voltage is slowly increased. In this process the microdischarge activities become more intense up the breakdown occurrence.
The higher the rate of X-rays bursts, the longer the duration between each cluster of microdischarges.

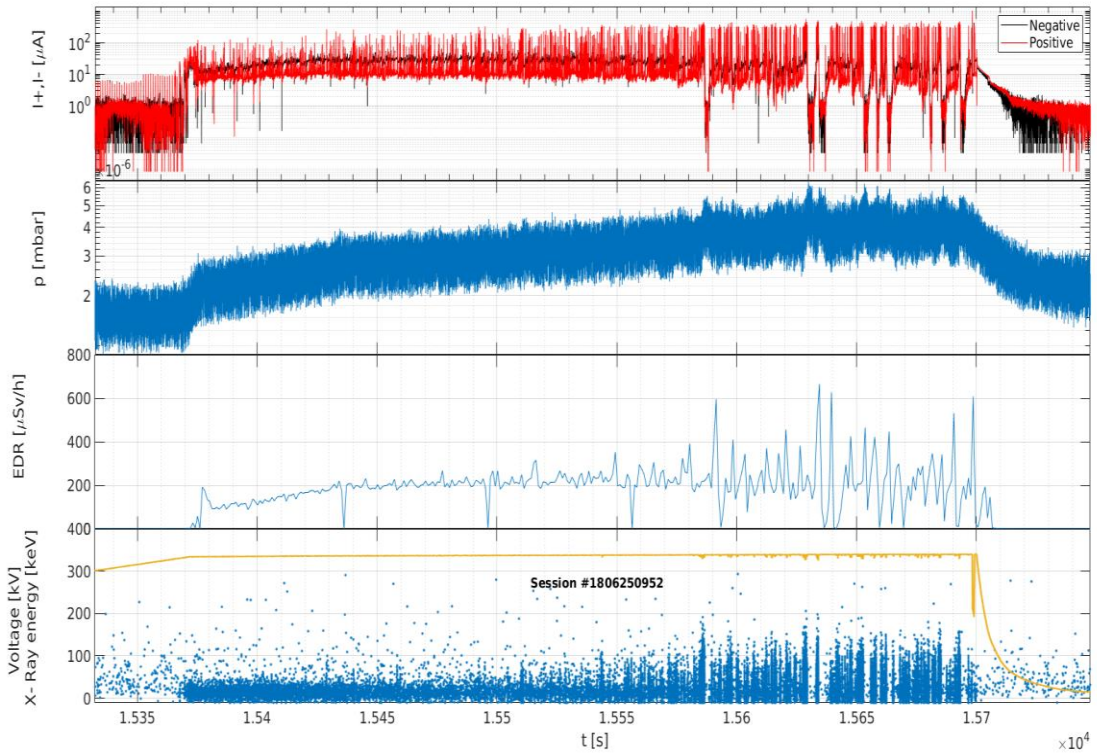

Figure 7- Overview of the typical time evolution of the quantities measured at the HVPTF. Data refer to condition C#1 of Table 1. Plot a) Ipos (red) Ineg (black) [mA], b) X-Ray counting rate [Hz], c) pressure [mbar], d) Applied voltage between electrodes [kV] , e) X ray energies.

Zooming progressively to smaller time windows, as shown in Figure 8, it is possible to observe that the duration of a single X-ray burst is in the range of 1-2 ms whereas the corresponding currents Ipos and Ineg last for longer periods of several tens of ms.

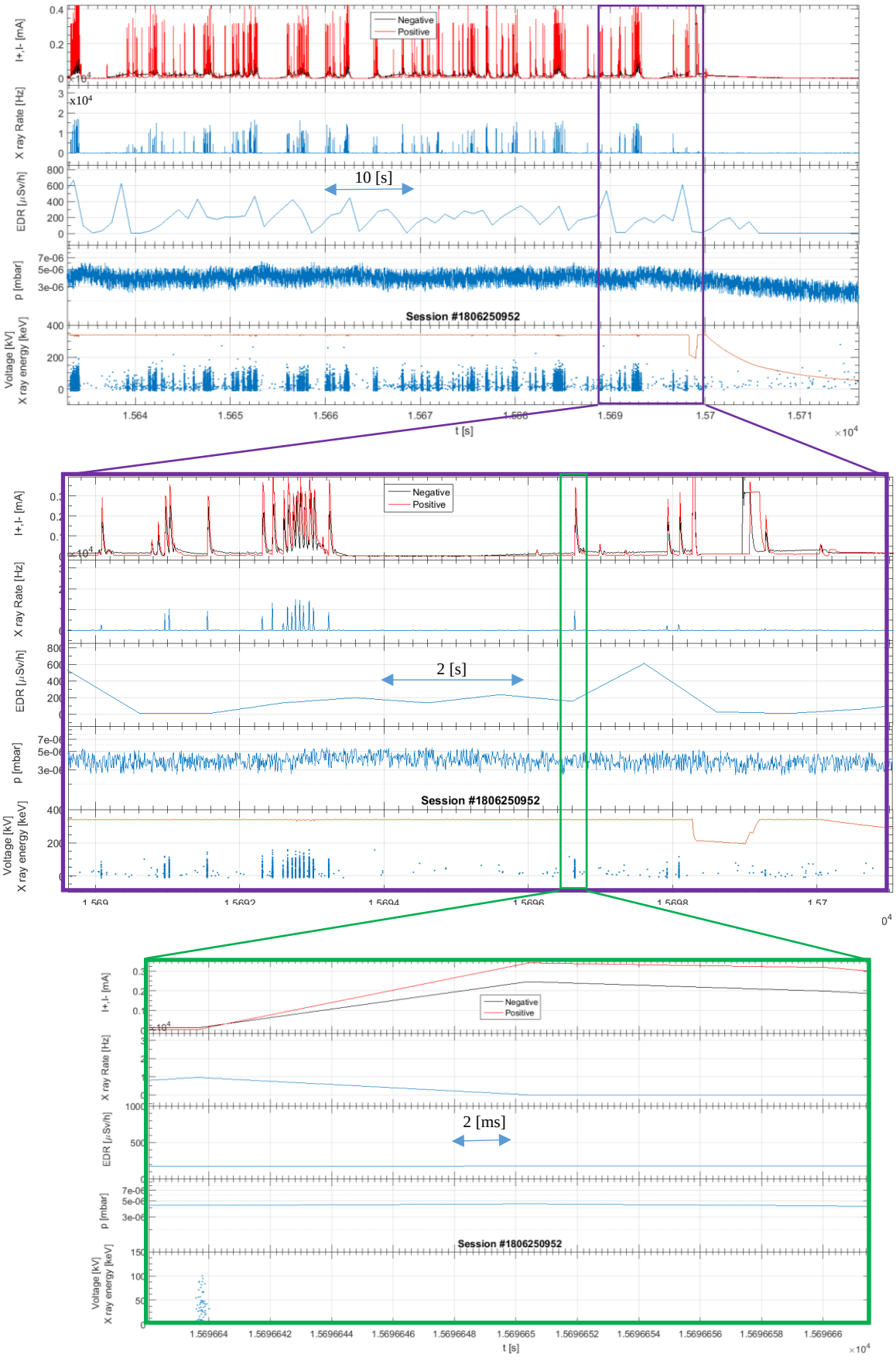

Figure 8. Typical time evolution of the quantities measured at the HVPTF. The data refer to condition C#1 of Table I.

Figure 7 reports the conditioning histories of the four experiments. In all cases, after 100/150 breakdowns the maximum voltage is reached. Referring to configuration #3, after breakdown #196 the positive feedthrough has been punctured with a measurable leak of SF_6 into the vacuum, and the pressure changed from 5e-07 mbar to 5e-06 mbar. After such an event, an evident voltage holding degradation occurred, with no chance of recovering.
The general comparison between configurations #1, #2 and #3 (same electrode geometries, but increasing gap) shows that the larger the gap the higher the voltage, although the cases with 72 and 147 mm seem to reach the end of the voltage conditioning at the same voltage level.
The comparison between configurations #1 and #4, which have almost the same gap length but different electric fields, shows that configuration #4 has a conditioning history with the voltages.
Configuration #4 exhibits the most relevant degradation of the voltage holding during the nights when the voltage is not applied.

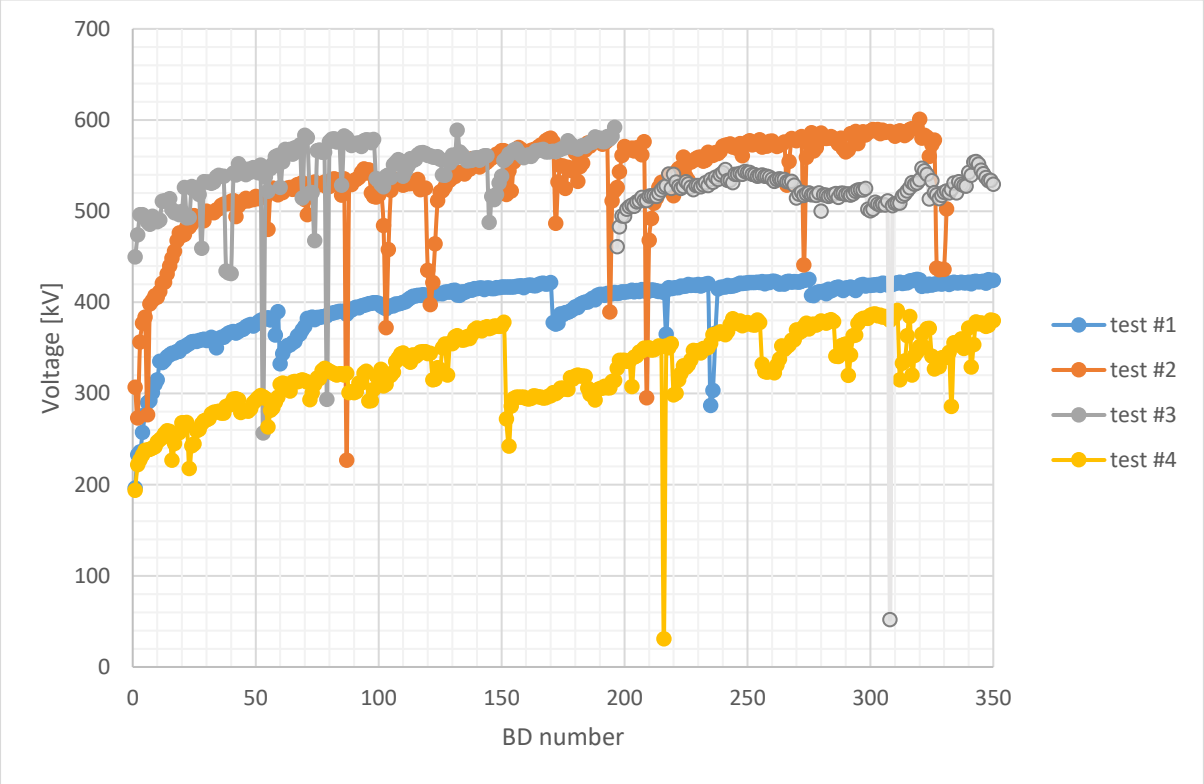

Figure 9. Conditioning histories during tests #1, #2, #3 and #4 as described in Table 1: breakdown voltages vs. progressive number. For test #3 the points recorded after the feedthrough puncture are highlighted in light grey.

1.1 The pressure effect

An example of a test in medium vacuum is shown in Figure 10, the measured quantities vs time are reported for configuration #3.
The test for the "pressure effect" started at t > 34000 s by injecting Argon into the vacuum vessel. The maximum available voltage 800 kVdc was achieved at 9 10^{-4} mbar, and an endurance test at 780kVdc with a pressure of 1.1 10^{-3} mbar was carried out for 10 minutes.

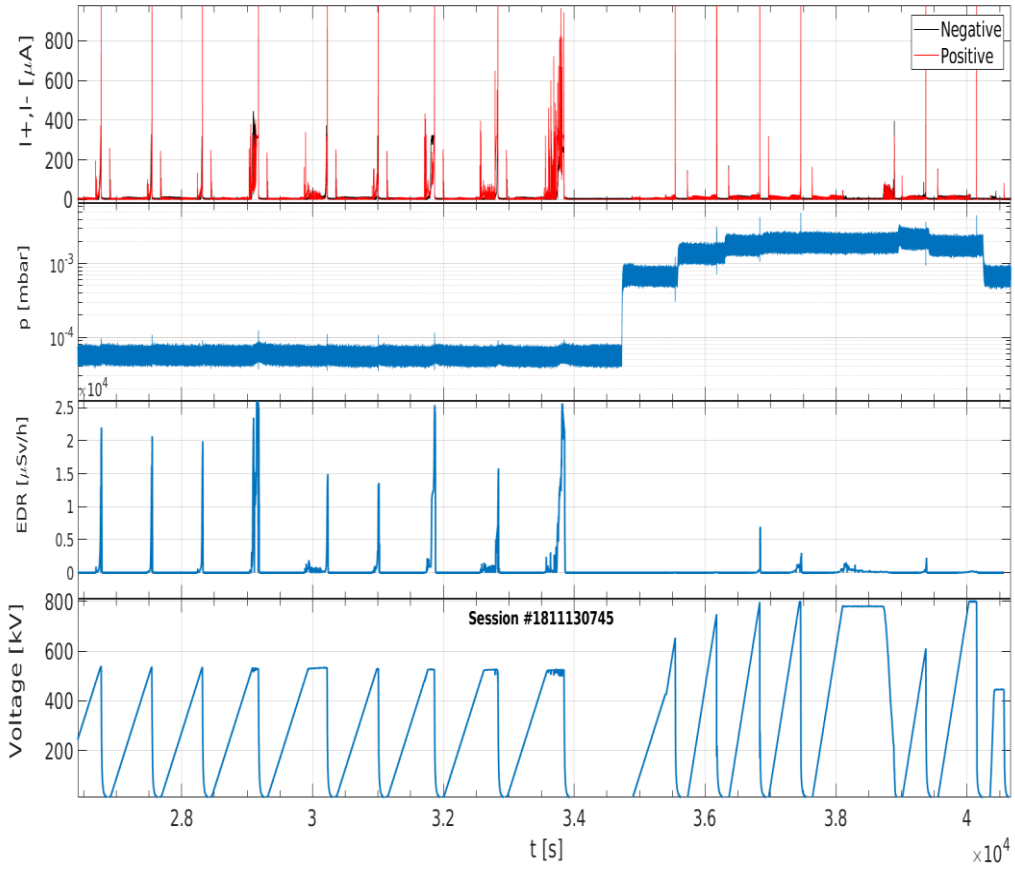

Figure 10. Time evolution of the measured quantities for test #3 during the achievement of the best hold off voltage performances.

Results of the pressure effect in Argon for each configuration of table I are reported in Figure 10. The colors of the plots coincide with those of Figure 9.

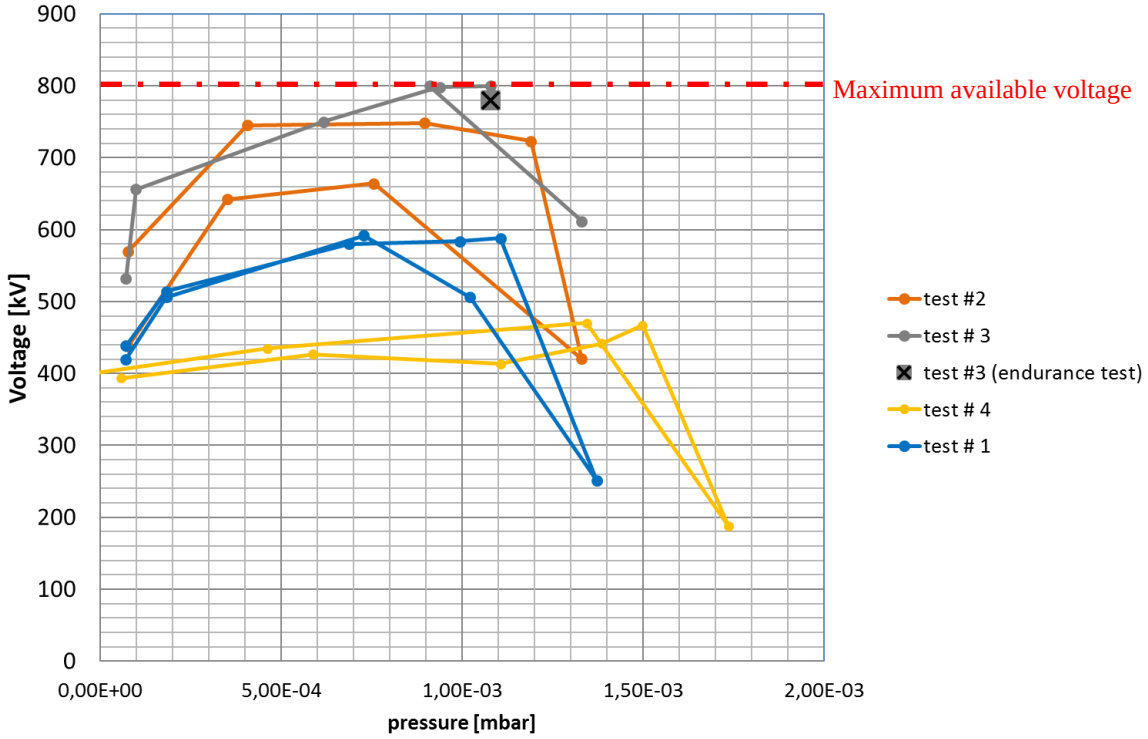

Figure 11. Systematic study of the pressure effect in Argon for tests #1, 2, 3 and 4. All the points refer to breakdown voltages except for the endurance test #3 where the 780 kV voltage at 1.08 10^{-3} mbar has been held for 10 minutes without breakdown.

4. Discussion

4.1 Current burst evolution

Referring to fig. 6, the phenomenology is dominated by the occurrence of a huge number of microdischarges appearing as a current burst of some hundreds of μA; these are measured independently by the positive and negative current probes, built-in to the two PSs. Although the higher electric fields and the highest voltage in vacuum are between the electrodes under test, the presence of spurious phenomena involving a mutual exchange of charged particles with the vacuum vessel was demonstrated in [23]. Nevertheless the contemporary presence of I_{pos} and I_{neg} and the relative position of the breakdown histories shown in Figure 9 indicates that the breakdown occurs between the electrodes under test.

As shown in [24] [25], if the voltage is kept constant, over a period of time the current bursts become less frequent until (almost) disappearing.

Most of the time the microdischarges are accompanied by gas emission and X-rays. X-ray energy spectra have been analyzed in detail in [26]

The high rate of X-rays produced during the HV conditioning was recorded by the PVT scintillator up to 300 - 400kHz. The NaI scintillator has proved not suitable due to excessive pile-up. Work is ongoing to identify the best scintillator material and geometry. The energy spectra recorded by the PVT scintillator, of the present experimental campaigns, are affected by single Compton Scattering rather than photoelectric adsorption [27] this leads to energy spectra with a negative slope having a huge number of counts at low energy and few counts at higher energy. Nevertheless, it is very interesting to observe that, during the microdischarge, there is a corresponding X-ray emission at the beginning of the current burst, lasting about one-two milliseconds. Such an X-ray burst corresponds to the initial, fast (timescale of nanoseconds) discharge across the gap. This discharge can't be measured by the current probe of the PS, mainly because it doesn't have sufficient bandwidth, and in any case can't detect the fraction of the microdischarge current between the electrodes (see Fig. 3).

It's worth noticing that (see Figure 8) the X-ray emission disappears after a few milliseconds even if the burst of currents lasts for several tens of ms. This is the clue that initially the current is started by electron bursts emitted by the cathode (producing the highest energy X-rays). Then the electron current flowing through the electrodes is chopped due the collapse of the voltage across the gap; this behavior can be simulated by a simple circuit analysis

where it is possible to observe a time constant of the measured currents (I_{pos} , I_{neg}) compatible with the product $C_1 \cdot (R_1+R_2)$=6ms.

4.2 Voltage Conditioning

Referring to Figure 9, two main observations can be made:

i) the voltage conditioning curve of case #1 is definitely much more regular than in case of longer gaps (#2 and #3), as well as in case #4, which has almost the same gap length, but the anode is spherical and not planar;

ii) ii) the two tests #2 and #3, despite that the gap lengths are 72 and 147 mm respectively, reach almost the same maximum breakdown voltage (in case #3, the voltage after the BD #196 is even lower than #2, but this is due to the damage of the feedthrough as mentioned).

To give an interpretation, the analysis of the conditioning process has been done in terms of the cathode and anode electric field and by applying the Voltage Holding Predictive Model [4] to the four cases.

4.2.1 Electric Field Analysis

The electric fields have been evaluated calculating the shape factors at the cathode and the anode, through eqs 1) and 2)

$$\boldsymbol{E_C = f_C \cdot \frac{V}{d}} \qquad (1)$$

$$\boldsymbol{E_A = f_A \cdot \frac{V}{d}} \qquad (2)$$

d being the gap length.
Table II shows the shape factor for the four configurations:

Table II - Shape factors for the four configuration

Test #	Gap length [mm]	f_C	f_A
1	33	2.08	0.71
2	72	2.92	0.78
3	147.5	4.05	1.11
4	30	1.94	1.94

It's worth noticing that the electric field at the anode in case #4 (sphere-sphere) is almost three times larger than the anode field of case #1 (sphere-plane).
With reference to Fig. 12, it is interesting to observe that the breakdown electric field at the cathode - at the very beginning of the conditioning phase - is the same for the four configurations: this does not appear for the anodic electric field.
This evidence would suggest that the HV conditioning would produce, at least during the first phases, a modification of the cathodic surfaces rather than on the anodes. Once the voltage conditioning is terminated, the Total Voltage Effect TVE, i.e. the energy of the particles exchanged between electrodes, plays a dominant role in determining the final hold-off voltage in high vacuum.

As expected, the anodic electric field for case #4 is by far the largest among the four cases. This is explained by the difference of geometries between cases #1 and #4; the larger scatter of breakdown voltages are likely to be associated to the processes (mainly outgassing) occurring at the anode - once it is hit by the electron bursts coming from cathode - amplified by a much larger electric field. The different scatter of the breakdown voltage between cases #1, #2 and #3 is instead depending on the higher energy of the electron bursts, accelerated by the higher voltage.

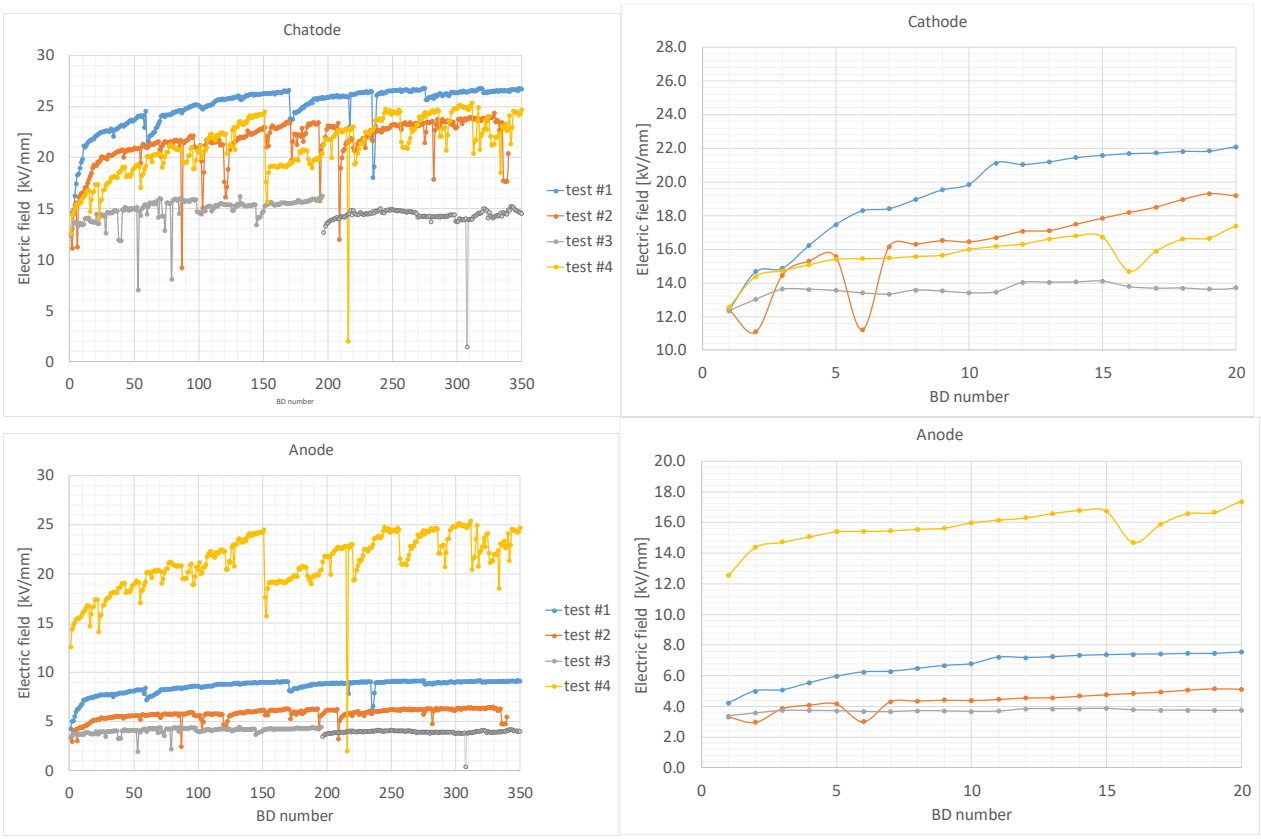

Figure 12. Cathodic and anodic electric field during HV conditioning vs. Breakdown number.

4.2.2 Application of the VHPM

The Voltage Holding Predictive Model VHPM has been applied to compare the measured breakdown voltage distribution for the four cases with the distribution calculated by the model.
The VHPM provides the breakdown probability *P* for any electrostatic system in high vacuum, calculated as:

$$P = 1 - exp\left[-\int \left(\frac{W-W_L}{W_0}\right)^m \cdot dA\right] \quad (4)$$

where

$$W = E_K^{\gamma} \cdot E_A^{\alpha} \cdot V \qquad 5)$$

The integral in formula 3) is extended to all cathodic surfaces and W is calculated using the local (cathodic) electric field and the anodic electric field E_A associated to E_K by a virtual particle leaving the cathode and colliding into the anode. V is the voltage between the departure and arrival points of the virtual particle. The parameters W_L, W_0, α and γ are independent of the electrode configuration, and have to be determined experimentally.
The comparison between the VHPM predictions and experimental results has been done using the parameters (W_0=2.0·10^8 (S.I. units), α=0.10 γ=0.3 and m=25) derived from an average of a relatively large database of electrostatic configurations, with gaps ranging from a few millimeters to 1.3 m [18]. The result is shown in Figure 13.

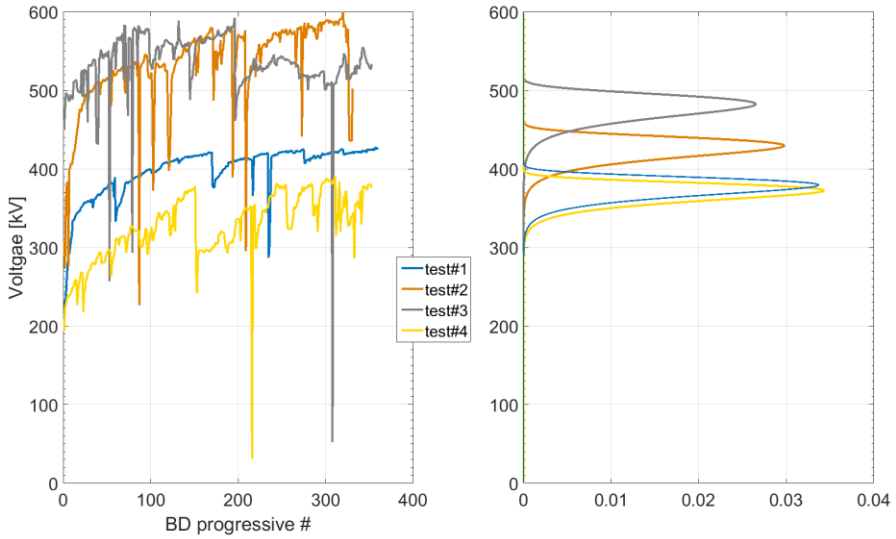

Figure 13. Comparison between the experimental breakdown voltage sequence and the breakdown probability density distribution predicted by the VHPM with W_0=2.0 10^8 α=0.1 γ=0.3 and m=25 (as reported in [28]). Predictions for cases #1 and #4 are almost coincident. Prediction #2 is clearly underestimated.

The last breakdown voltages of each curve shown in Figure 9 ,from BD #100 to the end of the conditioning (except for test #3 where only the voltages from the 100th to the 196th breakdown have been considered), have been used to calculate the density distributions of breakdown probability shown in plot a) of Figure 14.

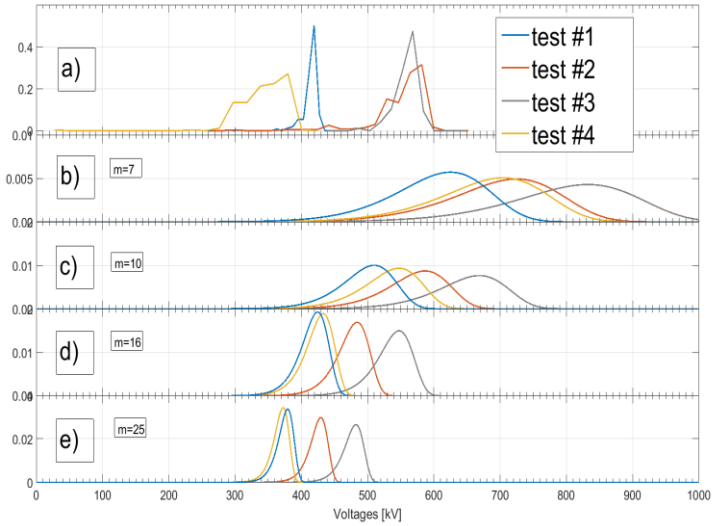

Figure 14. Experimental distribution of breakdown voltages, graph a), in comparison with numerically simulated voltage distributions calculated with different *m* parameters for W_0=1.98 10^8 (S.I. units) α=0.1 γ=0.29, as reported in [28].

For tests #1, #3 and #4, an agreement between results and prediction exists, even if it would appear marginal. Test #4 is well predicted, whilst the breakdown voltage for cases #1 and #3 is underestimated (the measure is outside the probability curve). On the other hand, the comparison of results from experiments which are nominally identical - e.g. having the same electrode material, geometry and pressure – but have been obtained from two different setups (and probably experimental procedure) can have differences of the hold-off voltage larger than 30% (see Fig. 11 of [29]).

In fact, the *m* parameter is not derived from the database of experiments considered in [28], but has been derived from the scattering of BD voltages from the single experiment reported in [30] so it doesn't take into account the relatively large scattering from the comparison of experimental results obtained from nominally identical setups.

It has been deemed interesting to make an analysis of the effect of m variation of the probability curves. Figure 14 shows the results: graph a) shows the measured probability distribution.
With m=16, the agreement improves for cases #1 and #3, but slightly worsens for #4.
Case #2 requires separate discussion. The underestimation of the numerical model is evident as Figure 9 shows that, at the end of the conditioning, the 72 mm gap holds the same voltage (almost 580kV) as the 147 mm gap.
In other words, the TVE observed in the experimental campaigns appears more marked than the one predicted by the numerical models.
So far, no explanation has been found for such an unexpected result; the next experimental campaigns aim to explore this issue.
An additional observation can be deduced from ref. [18] which reports an interesting experimental result of the Quantum Science Technology (QST) laboratory. The QST tested the dc voltage holding of a stainless steel sphere of radius 250 mm, connected to the negative polarity versus a stainless steel plane at ground potential, the pressure was lower than 10^{-6} mbar and the electrodes were separated by a very long gap length of 1290 mm. The maximum voltage at the end of conditioning in high vacuum was 705kVdc. Although this result was obtained adopting an experimental procedure and an electrode preparation different from the one reported in this paper, it confirms a strong saturation of the hold-off voltage vs gap length for voltages above 500-600kVdc in high vacuum.
Interesting information concerning the scaling law for the breakdown voltages can be obtained from eq. 4 considering configurations in "geometric similarity", i.e. configurations having a shape which correspond to a similar distribution of electrostatic fields in the vacuum insulation between cathode and anode.
If two configurations, labelled 1 and 2, have the same breakdown probability, then eq. 5 is satisfied:

$$\int \left(\frac{W_1}{W_0}\right)^m \cdot dA_1 = \int \left(\frac{W_2}{W_0}\right)^m \cdot dA_2 \qquad (6)$$

Considering eq. 1 to 5 it is possible to obtain eq. 6 which represents the relation between the breakdown voltages U_1 and U_2, for two configurations having the same shape at the same breakdown probability.

$$U_2 = U_1 \cdot \left(\frac{d_2}{d_1}\right)^{\left[\frac{\alpha+\gamma}{1+\alpha+\gamma} - \frac{2}{m\cdot(\alpha+\gamma+1)}\right]} \qquad (7)$$

In Figure 15, the ratio U_2/U_1 is represented as a function of the gap length ratio d_1/d_2, according to eq. 6, using the same parameter α=0.1 γ=0.3 as above described. The validity of this relationship is limited to the long gap cases, which correspond approximately to d_2 > 0.01 m. The short gap configurations have a breakdown voltage determined by the existence of a maximum electric field [20] [3], so in the case of a gap length of < 0.01 m the triple product of eq. 3 is no longer applicable and eq. 6 cannot be used.

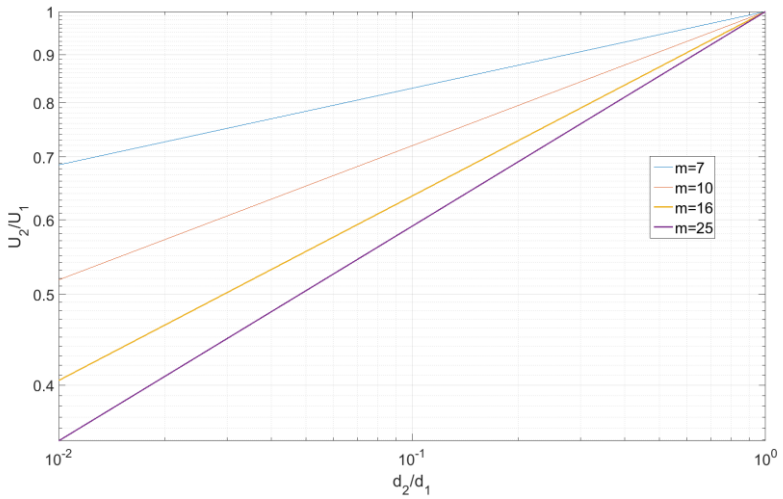

Figure 15. Plot of ratio U_2/U_1 as function of the gap length ratio d_2/d_1, for a sphere-plane configuration with *m*=16 and *m*=25, assuming α=0.1 and γ=0.29

It is interesting to observe that in the QST sphere-plane test configuration, the ratio d/R was 1300/250 ≈ 5.2, whereas in the HVPTF sphere-plane tests #1, #2 and #3, the ratio d/R was 30/20=1.5, 72/20=3.6 and 147.5/20=7.37, respectively. Therefore, in the HVPTF, a spherical electrode, R = 20 mm, separated by a gap length of d=104 mm (104/20=5.2) would be "geometrically similar" to the QST setup. Interpolating the experimental results shown in Figure 9, it seems plausible that, in HVPTF, such a sphere-plane configuration could have reached a final breakdown voltage in the range 500-600 kV, whereas we know that the QST setup has obtained a maximum voltage of 705 kV. Therefore, based on the real QST experiments and on the (interpolated) HVPTF experiments, the voltage ratio U_2/U_1 for these two "geometrically similar" configurations is in the range of between 0.71 (=500/705) to 0.85 (=600/705). This voltage ratio is fairly consistent with the value obtained for a gap length ratio d2/d1=104/1300 =0.08 from the plots in Figure 15, which indicate a voltage ratio U2/U1 in the range 0.56-0.82 (depending on m).
Based on this observation and on a comparison between the top plot of Figure 14 and the other ones in the same figure which indicate a best fit for m > 7, it seems that the optimal choice to improve the model predictions could be estimated as m=16.
As mentioned in [28], the derivation of the numerical model parameters requires a high number of experimental results. The statistical approach appears a fundamental tool to take into account the experimental results from different experimental setups. In fact, the definition of the voltage holding capability of a device insulated by high vacuum requires the specification of a number of boundary conditions to obtain a certain reproducibility of the experimental results.

*4.3 **P**ressure **E**ffect*

The experimental results reported in Table III and Figure 11 indicate that a considerable improvement can be achieved in the voltage holding capability by injecting small quantities of Ar into the vacuum, in this way the Pressure Effect (PE) allows to obtain the maximum available voltage. This results appears in agreement with those

reported in [21] where it was possible to sustain more than 1.5 MVdc with a vacuum gap of 200 mm and a pressure of 10^{-4} mbar in N_2.
Table III also compares the experimental results without gas, before and after conditioning, with the results obtained with gas. The comparison is carried out in terms of voltages and electric fields. As noted, PE is a technique known since the early fifties. Nevertheless, neither consolidated physical explanations nor reliable numerical models are presently available to predict numerically the voltage holding improvements. The experience reported in this paper indicates that it is possible to limit the electron current from the cathode by adding an external gas, this effect is evident when comparing the EDR signal in Figure 10 in high vacuum and during the PE test. The PE is also reversible: if the pressure of the external gas was slowly decreased during the endurance test at 780kV, shown in Figure 10, the EDR (and the X-ray rate) would quickly increase up to the occurrence of the breakdown.

Table III. Voltage holding capability obtained with and without gas for each configuration

Test #	Without gas						With gas				
	Before conditioning			After conditioning			Best performances – Pressure Effect				
	Ec_B	Ea_B	U_B	Ec_A	Ea_A	U_A	Ec_{PE}	Ea_{PE}	U_{PE}	$\frac{U_{pe}-U_A}{U_A}$	p*1e04
	[kV/mm]	[kV/mm]	[kV]	[kV/mm]	[kV/mm]	[kV]	[kV/mm]	[kV/mm]	[kV]		[mbar]
1	12.4	4.2	196	26.9	9.2	426	37.3	12.7	592	**49%**	7
2	12.4	3.3	307	20.4	5.4	502	30	8.0	748	**39%**	4- 9
3	12.3	3.4	450	14.6	4	533	22	6.0	800	**>50%**	9
4	12.5	12.5	193	24.4	24.4	376	30.4	30.5	470	**25%**	13.5

According to the experimental results above, the improvement of voltage holding with gas is in the range of +25% to 50 % between the highest voltages and the corresponding values after conditioning in high vacuum. Higher improvements of voltage holding have been observed in tests #2 and #3 which are the experiments with the longest gap lengths, which is in line with the results reported in [17] and [20].
The pressure corresponding to the best voltage holding capability improvement is closer to 5 10^{-4} mbar. This is of great interest for the MITICA accelerator because the pressure at the Beam Source during the beam extraction is around the same value [11] [9]. In any case, further experimental investigations are necessary to clarify this aspect.

Conclusions

The results of the experimental campaign presented in this paper constitute an investigation aimed to clarify physical and technical aspects concerning the initiation and the development of electrical breakdown across long vacuum gaps. The breakdown across long vacuum gaps is one of the most critical aspects concerning the 1 MVdc insulation system for the ITER Neutral Beam Injector. The investigation was limited to the first and the third working conditions mentioned in the introduction (DC voltage applied in high vacuum or in low-pressure gas, zero RF voltage applied). The main outcomes are the following.
An accurate control of the status of the electrode surfaces and the adoption of an automatic conditioning procedure have allowed to evaluate and compare the conditioning histories of four different electrode geometries. The breakdown electric field at the cathode, observed at the very beginning of the conditioning phase, is always the same irrespective of the studied geometry: this is not the case for the anodic electric fields. This fact seems to imply that the HV conditioning would produce, at least during the first phases, a modification of the cathodic metal-vacuum interfaces rather than of the anodic interfaces.
The benchmark between VHPM and the experimental results obtained in four different experimental setups has shown a relatively good agreement between the model predictions and the previous experimental observations. Nevertheless, the validation process and the improvement of the probabilistic model still remain ongoing activities that need experimental data, especially from configurations having long vacuum gaps and large electrode areas.
The use of Time-Correlated Single Photon Counting (TCSPC) techniques has revealed a valid tool to monitor the HV conditioning in terms of pre-breakdown currents and microdischarge activity. On this basis, the combination of TCSPC with the a pressure measurement and RGA signals can be considered as a suitable method to monitor

the HV conditioning of the electrostatic accelerator in MITICA, where the minimum detectable current of the HV Power Supplies (tens of milliamperes) is too high to recognize if HV conditioning is occurring.
The tests reported in this paper confirm the existence of a marked total voltage effect: for gap length larger than 70 mm it was not possible to sustain more than 600kVdc in high vacuum, approximately the same maximum voltage was sustained by a 148 mm gap. This result , obtained using stainless steel electrodes having clean, regular surfaces and relatively small areas, is consistent with the predictions reported in [15] and with the more recent analyses and experimental results of [18] [31].
Studies of alternative methods to improve the hold-off voltages for large gaps in high vacuum still remain an ongoing activity. The best-known option to improve the hold-off voltage in high vacuum is the adoption of multiple nested screens structures, where each screen is connected to the intermediate voltages. Although the effectiveness of such a solution has already been tested in the past [19] [18], it has relevant drawbacks considering the requirement on pumping the gas flowing out of the beam source, and also the beam tilting and the remote handling maintenance, as foreseen in ITER [32].
The experiments reported in the present paper also confirmed the existence of a pressure effect, demonstrating that it is possible to sustain 780kVdc in a gap of 150 mm for several minutes, at a pressures of a few 10^{-4} mbar. This pressure effect appears to be compatible with the pressure levels foreseen in MITICA during the beam operation. However, the improvement due to the pressure effect does not have consolidated physical explanations, even though it is well documented in literature [21]
By scaling these results, it seems that the injection of H2 could improve the voltage holding in MITICA geometry up to 1MVdc without any design modifications. However, the pressure surrounding the BS depends on the pressure of the RF plasma source. In practice, the complexity of the system geometry and of the operation modes makes the commissioning of the full scale accelerator prototype the only meaningful test to verify the effectiveness of any solutions to improve the hold-off voltage of the MITICA electrostatic accelerator.

Acknowledgments

The work leading to this publication has been funded partially by Fusion for Energy. This publication reflects the views only of the authors, and F4E cannot be held responsible for any use which may be made of the information contained therein. The views and opinions expressed herein do not necessarily reflect those of the ITER Organization.

References

[1] V. Toigo et. Al. “The PRIMA Test Facility: SPIDER and MITICA test-beds for ITER neutral beam injectors” New Journal of Physics vol. 19, No. 8, (2017)

[2] De Lorenzi et. Al. “HVPTF—The high voltage laboratory for the ITER Neutral Beam test facility” Fusion Engineering and Design Vol. 86, No.. 6–8, pp 742-745, (2011)

[3] F. Rohrbach “Isolation sous Vide” ,CERN Report 71-5, (1971).

[4] N. Pilan, P. Veltri and A. De Lorenzi “Voltage Holding Prediction in Multi Electrode–multi Voltage Systems Insulated in Vacuum” IEEE Transactions on Dielectrics and Electrical Insulation Vol. 18, No. 2; April (2011)

[5] DeEsch et. Al. Nucl. Fusion 55 096001 (2015)

[6] R S Hemsworth et al New J. Phys. 19 025005 (2017)

[7] Fantz U et al Towards 20 A negative hydrogen ion beams for up to 1 h: achievements of the ELISE test facility Rev. Sci. Instrum. 87 02B307 (2016)

[8] A. Kojima et Al. “Achievement of 500 keV negativeion beam acceleration on JT-60Unegative-ion-based neutral beam injector” Nucl. Fusion 51 083049 (8pp) , (2011)

[9] ITER Technical Basis 2002 Neutral beam heating and current drive (NB H a ndCD) system detailed design document (section 5.3, DDD5.3) (Vienna: IAEA)

[10] P. L. Mondino et al., Nucl. Fusion 40, 501 (2000).

[11] E. Sartori et Al. “Distribution of the background gas in the MITICA accelerator” AIP Conference Proceedings 1515, 121 (2013)

[12] N. Pilan, G. Chitarin, A. De Lorenzi and G. Serianni “Magnetic field effect on Voltage Holding in the MITICA Electrostatic Accelerator” IEEE Tran. On Pla. Sci. Vol. 42 , No.2, (2014)

[13] G. Serianni et. Al. “First operation in SPIDER and the path to complete MITICA" , to be published in Review Sci. Instriments

[14] Takeiri et. Al. “Development of a high-current hydrogen-negative ion source for LHD-NBI system” NIFS—557 (1998)

[15] N. Pilan et. Al. “Voltage holding optimization of the MITICA electrostatic accelerator” Fusion Engineering and Design Vol. 88, No.. 6–8, Pages 1038-1041, (2013)

[16] T. Patton et. Al “MITICA intermediate electrostatic shield: Concept design, development, and first experimental tests identification” AIP Conference Proceedings 2052, 030002 (2018)

[17] Latham R High Voltage Vacuum Insulation (San Diego, CA: Academic) Ch. 2 (1995)

[18] A. Kojima et al “Demonstration of 1 MV insulation for the vacuum insulated beam source in the ITER neutral beam system “Nucl. Fusion 59 086042 (2019)

[19] A. A. Kudryavtsev, et. Al. “First experimental results from 2MeV proton tandem accelerator for neutron production” Rev Sci Instrum. vol 79, 02C709 (2008)

[20] C. Germain, F. Rohrbach “High voltage breakdown in vacuum” Vacuum Volume 18, Issue 7, pp 371-377, (1968)

[21] K. W. Arnold et. Al. “Electrical Breakdown between a sphere and a plane in vacuum” Proceedings of Sixth International Conference on Ionization phenomena in gases on lonization Phenomena in Gases, Paris 2 . 101- 4 (1963)

[22] Yasushi Yamano “Vacuum Breakdown Characteristics for Stainless Steel Electrode and Influence of Contamination Degree of the Electrode Surface on the Breakdown Characteristics” proc. 1st International Conference on Electric Power Equipment – Switching Technology – Xi’an – China (2011)

[23] N. Pilan et Al. “Evidences of accumulation points in cascade regenerative phenomena observed in high voltage dc devices insulated by long vacuum gaps” J. Phys. Commun. 2 115002 (2018)

[24] Spada et Al. “Theoretical Basis and Experimental Validation of the Breakdown Induced by Rupture of Dielectric Layer Model” IEEE Tran. On Pla. Sci. Vol. 47 , No.5, (2019)

[25] H. P. S. Powel and P. A. Chatterton “Prebreakdown conduction between vacuum insulated electrodes” Vacuum , vol. 20 -10 , (1970)

[26] Spagnolo “Current Signals and X- Ray Spectra Analysis for a Vacuum High Voltage Holding Experiment” Proceeding of the 28th International Symposium on Discharges and Electrical Insulation in Vacuum, Volume 1, pp 89-92, (2018)

[27] Siciliano, E. R et. Al. , “Energy calibration of gamma spectra in plastic scintillators using Compton kinematics” S. T. Nuclear Instruments and Methods in Physics Research Section A, Volume 594, Issue 2, p. 232-243 (2008)

[28] N. Pilan et Al. “Numerical-Experimental Benchmarking of a Probabilistic Code for Prediction of Voltage Holding in High Vacuum” IEEE Tran. On Pla. Sci. doi: 10.1109/TPS.2017.2775246 (2017)

[29] F. Rohrbach “Isolation sous Vide” ,CERN Report 71-5, (1971).

[30] De Lorenzi et. Al. “Progress in the Validation of the Voltage Holding Prediction Model at the High-Voltage Padova Test Facility” IEEE Tran. On Pla. Sci. Vol. 41 , No.8, (2013)

[31] Nishimori N, Nagai R, Matsuba S and Hajima R Phys. Rev. S. T. Accel. Beams 17 053401 (2014)

[32] Choi C-H et al 2011 Remote handling concept for the neutral beam system Fusion Eng. Des. 86 2025–8